

# MEASUREMENTS OF DECAY RADIOACTIVITY OF LONG-LIVED ISOTOPES

A. Kumar, M.A. Abdou, M.Z. Youssef  
School of Engineering and Applied Science  
University of California at Los Angeles  
Los Angeles, CA 90024-1597  
310-825-8627

Y. Ikeda, C. Konno, Y. Oyama,  
K. Kosako, F. Maekawa, H. Maekawa  
Department of Reactor Engineering  
Japan Atomic Energy Research Institute  
Tokai, Ibaraki 319-11, Japan  
011-81-292-82-6016

## ABSTRACT

Measurements of long-lived radioactivity are required to generate reliable data-base for qualifying fusion materials for reactor applications. However, long half lives necessitate intense 14 MeV neutron source, long irradiation time, long cooling time, and long counting time under low background. A 32h12m long irradiation, at mean source neutron intensity of  $1.13 \times 10^{12}$  n/s, was carried out on a number of foil packages kept near rotating neutron target source at FNS under USDOE/JAERI collaborative program in June 1989. Four identical foil packages were kept at 0, 45, 90, and  $\sim 115$  degrees to the  $d^+$  beam. Each package contained foils of Ag, Al, Dy, Hf,  $^{151}\text{Eu}$ ,  $^{153}\text{Eu}$ , Hf, Ho, Ir, Mo, Re, Tb, and W. The objective was to measure decay  $\gamma$  radioactivity from  $^{108m}\text{Ag}$ ,  $^{26}\text{Al}$ ,  $^{158}\text{Tb}$ ,  $^{152}\text{Eu}$ ,  $^{150}\text{Eu}$ ,  $^{94}\text{Nb}$ ,  $^{186m}\text{Re}$ ,  $^{178m2}\text{Hf}$ ,  $^{192m}\text{Ir}$ , and  $^{166m}\text{Ho}$ , among others. The half lives of these products range from 13.3y ( $^{152}\text{Eu}$ ) to 0.72My ( $^{26}\text{Al}$ ). These foils were interspersed with dosimetric foils of Nb and Zr. An estimated average fluence of  $\sim 0.83 \times 10^{15}$  n/cm<sup>2</sup> (range: 0.47-1.65.10<sup>15</sup> n/cm<sup>2</sup>) was obtained for the foil-package at zero degree. After cooling times ranging from 1.3 to 2 years,  $\gamma$ -spectroscopy of some of these foils has been completed. Analysis of measurements, done on foil package at zero degree, has been carried out using four radioactivity codes, REAC-2, DKRICF, ACT4 (THIDA-2), and RACC. REAC-2 is the only code that has data for most of the observed products; RACC has data for Al, Mo and W products only. Ratio of computed to experimentally measured activities varies from  $4 \cdot 10^{-5}$  to 377. Major update of all four cross-section libraries is recommended as waste classification of many fusion specific materials is likely to change dramatically.

## I. INTRODUCTION

Materials in fusion reactors will generate a variety of long-lived radioactive isotopes due to their exposure to high 14 MeV neutron fluxes. These long-lived isotopes raise serious concern regarding waste disposal, maintenance, and safety<sup>1-6</sup>. Nuclear data base for these isotopes is scarce. Calculations by theoretical models have not either been attempted frequently enough or are not very satisfactory<sup>6</sup>. They are subject to many uncertainties as even basic nuclear level properties are not available for many long-lived isotopes. Hence, measurements of long-lived radioactivity are required to generate reliable data-base for qualifying fusion materials for reactor applications. However, long half lives necessitate intense 14 MeV neutron source, long irradiation time, long cooling time, and long counting time under low background.

Requirements for activation cross section data for fusion reactors were outlined recently by Cheng<sup>2,7</sup>. Among the cross sections recommended to be measured included:  $^{95}\text{Nb}(n,2n)^{94}\text{Nb}$

( $t_{1/2}=20.3\text{Ky}$ ),  $^{109}\text{Ag}(n,2n)^{108m}\text{Ag}(127\text{y})$ ,  $^{151}\text{Eu}(n,2n)^{150}\text{Eu}(35.8\text{y})$ ,  $^{153}\text{Eu}(n,2n)^{152}\text{Eu}(13.3\text{y})$ ,  $^{158}\text{Dy}(n,p)^{158}\text{Tb}(150\text{y})$ ,  $^{193}\text{Ir}(n,2n)^{192m}\text{Ir}(241\text{y})$ ,  $^{182}\text{W}(n,n'\alpha)^{178m2}\text{Hf}(31\text{y})$ ,  $^{187}\text{Re}(n,2n)^{186m}\text{Re}(0.2\text{My})$ ,  $^{179}\text{Hf}(n,2n)^{178m2}\text{Hf}(31\text{y})$ ,  $^{185}\text{Re}(n,\gamma)^{186m}\text{Re}(0.2\text{My})$ ,  $^{151}\text{Eu}(n,\gamma)^{152}\text{Eu}(13.3\text{y})$ ,  $^{165}\text{Ho}(n,\gamma)^{166m}\text{Ho}(1.2\text{Ky})$ , and  $^{191}\text{Ir}(n,\gamma)^{192m}\text{Ir}(241\text{y})$ . Only, recently, there has been a coordinated effort by an IAEA CRP (Coordinated Research Program) to get these and other cross sections measured. Prior work in this area has been reviewed by Qaim<sup>6</sup>, and is mostly available in references 8 through 13.

A long irradiation for decay  $\gamma$  radioactivity measurements was carried out at fusion neutronics source facility of JAERI in June 1989, under USDOE/JAERI collaborative program, to respond to the pressing need for providing activation cross sections for long-lived isotopes, on one hand, and validation of existing data-bases of leading radioactivity-calculation codes, on the other. Preliminary data on measured activation cross sections was recently reported elsewhere<sup>14</sup>. This complements our concurrent program on short-lived isotopes, within the same framework, that has led us to uncover large discrepancies on activation cross sections and decay data for a number of materials, e.g., Ni, Mn, Mo, Ti, Zr, W, Ta, Zn, Sn, Cr, Pb, V, and Co<sup>15-17</sup>. Here, we present and discuss measured decay  $\gamma$  radioactivity data for 11 materials irradiated at zero degree orientation with respect to  $d^+$  beam axis. Results of analysis using four leading radioactivity codes are subsequently discussed.

## II. EXPERIMENT

Figure 1 shows experimental arrangement of four foil packages near rotating neutron target (RNT) of fusion neutronics source(FNS) facility of JAERI. Arrangement of foils inside foil package#1 (0 degree) is provided in Figure 2. Irradiation data is summarized in Table I. 14 MeV neutron flux inside each foil package was monitored through  $^{93}\text{Nb}(n,2n)^{92m}\text{Nb}$  reaction by placing 10 Nb foils, a Nb foil separating two main foils. Zr foils were also kept, only 5 of them per package. The objective behind the latter foils was to monitor neutron energy spectrum through Zr/Nb activity ratio. However,  $^{90}\text{Zr}(n,2n)^{89m+8}\text{Zr}$  ( $t_{1/2}=78.4\text{h}$ ) reaction rate could not be measured due to strong interference from longer half life isotopes from the same material. The first Nb foil (Nb-1 in Fig. 2) is deduced to be at 2.51 cm from the source point (inside target) from the measured  $^{92m}\text{Nb}$  activity. Mean 14 MeV neutron fluence over package#1, spread over a distance of 2.51 to 4.69 cm from the source point, is estimated to be  $\sim 0.83 \cdot 10^{15}$  n/cm<sup>2</sup>, for irradiation of 32h12m duration at averaged source intensity of  $1.13 \cdot 10^{12}$  n/s. The fluence over this package is deduced to range from  $1.65 \cdot 10^{15}$  to

0.47.10<sup>15</sup> n/cm<sup>2</sup>.

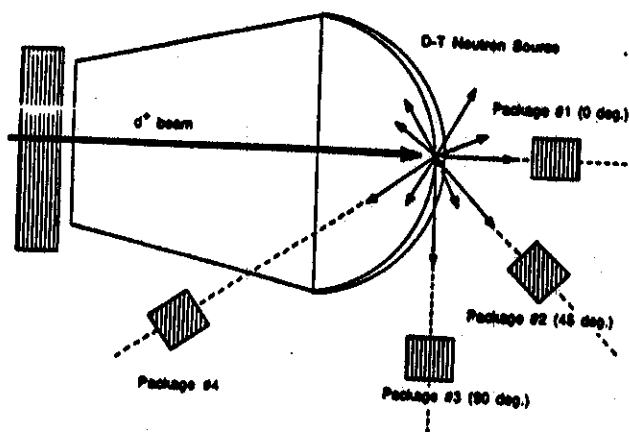


Fig. 1. FNS rotating neutron target and irradiation configuration

TABLE I

Long-lived Radioactivity Experiment: Irradiation Data

14 MeV Source:  
 Fusion Neutronics Source (FNS) at JAERI  
 D-T Neutrons via <sup>3</sup>T(d,n)<sup>4</sup>He Reaction  
 Deuteron energy: 350 keV  
 Average d<sup>+</sup> beam current: 20 mA  
 Typical Sample size:  
 10 mm in dia x 1-2 mm in thickness  
 10 mm x 10 mm x 1 mm  
 Sample position:  
 0, 45, 90 deg. with respect to d<sup>+</sup> beam  
 at 3 - 5 cm from the target  
 Flux Monitor: <sup>93</sup>Nb(n,2n)<sup>92m</sup>Nb  
 Irradiation time: 32 hours  
 Average Neutron Intensity: 1.13 x 10<sup>12</sup> n/s

Large volume germanium detector, with 115% efficiency relative to NaI(Tl), was employed for  $\gamma$ -spectroscopy after an initial cooling period of more than 1.4 y. Long cooling times are needed for elimination of strongly interfering decay  $\gamma$ s from short-lived isotopes. 184 KeV  $\gamma$  from <sup>166m</sup>Ho (t<sub>1/2</sub>=1200y) was not observed due to its decay rate being quite low; quite possibly, it is overwhelmed by much higher background count rate. Typical cooling and counting times for eleven foils of package#1 are displayed in Table II. Cooling times varying from 1.47 to 1.99y and counting times varying from 103.8 m to 13945.8 m are involved. Major impurities are also listed in the same table. Hafnium and dysprosium have largest impurity contents. The count data was analyzed using spectroscopy application package, of Nuclear Data Systems, which was installed on newly introduced Vax station 3100M48-based data-acquisition system (including ND556 acquisition interface module) at FNS. This gave peak energy, counts, and standard deviation on counts. As expected, large number of  $\gamma$ -peaks are due to background. Visual peak identification is a must.

The identified peaks with their percent decay yield and half life data, from references 18 and 19, are shown in Table III. A large number of peaks are observed for <sup>110m</sup>Ag, <sup>154</sup>Eu, <sup>152</sup>Eu, <sup>150</sup>Eu, <sup>173</sup>Lu, <sup>178m2</sup>Hf (from Hf), <sup>192</sup>Ir, <sup>184</sup>Re, <sup>182</sup>Ta,

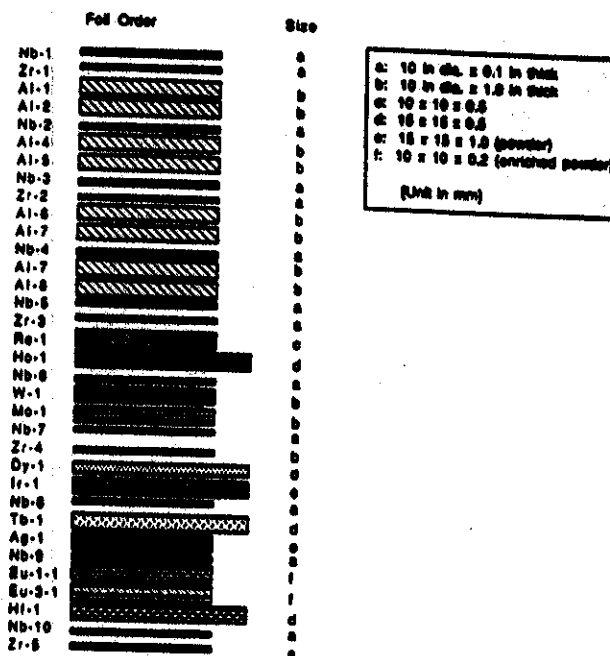


Fig. 2. Foil arrangement within foil package#1

TABLE II

Cooling and Counting Times for Foil Packet at Zero Degree

Material	Major Impurities (Maximum Weight % or ppm)	Identifier	Cooling Time	Counting Time
Ag	<0.01% (Au: 10ppm)	AGLL1	1.83y	436.76m
Al	<0.01%	ALLL2	1.99y	13946.34m
Dy	0.6%Ta, 0.01%Tb/Ho/Gd/Er	DYLL4	1.82y	3843.34m
97.7% <sup>151</sup> Eu	2.8% <sup>153</sup> Eu	EUS13	1.85y	987.83m
99.2% <sup>152</sup> Eu	0.8% <sup>151</sup> Eu	EUS32	1.85y	4411.95m
Hf	<3%Zr:2.8%Ta:100%Fe:100%Nb:30%W:30	HFLL2	1.34y	3358.84m
Ir	<0.1%Rh:200%Fe:30%Pb:30%Pt:20%Pd:20	IRLL1	1.82y	283.10m
Mo	<0.1%Fe:30%Cr:30%Cu:20%Pb:30	MOLL2	1.52y	13945.76m
Re	<0.01%Fe:45%Mo:30%Co:3%Zr:2%Mn:2	RELL1	1.47y	1294.71m
Tb	0.1%Ta:0.01%Eu/Dy/Gd/Y	TBLL1	1.82y	103.82m
W	<0.03%:0.008%Si	WILL2	1.51y	2450.70m

<sup>184m</sup>Re, <sup>160</sup>Tb (Tb & Dy), and <sup>158</sup>Tb(Tb). However, no peaks were observed for <sup>192m</sup>Ir(241y), <sup>186m</sup>Re, and <sup>178m2</sup>Hf (31y, from W). Probable reason lies in their low activation cross sections and decay  $\gamma$  yields. Nuclear reactions considered responsible for these observed peaks are summarized in Table IV. 'IT' stands for isomeric transition. <sup>94m</sup>Nb is not listed in Table IV. It has a half life of 6.26m and decays into <sup>94</sup>Nb via IT with 99.53% branching ratio<sup>18</sup>.

TABLE III

Radioactive Products and Prominent  $\gamma$ -ray Peaks Observed in Experiment on Long-lived Isotopes Production in Fusion Neutron Environment

Irradiated Material	Products/yield & $\gamma$ -ray energy (KeV)	Irradiated Material	Products/yield & $\gamma$ -ray energy (KeV)
Ag	249.8d $^{110m}\text{Ag}$ : 94.6% 658/10.4% 678/6.4% 687/16.4% 707/4.7% 744/22.3% 764/7.3% 818/72.7% 885/34.4% 937/24.3% 1384/4.0% 1476/13% 1505 127y $^{108m}\text{Ag}$ : 0.5% 434/0.3% 619/1.8% 633 2.37m $^{108}\text{Ag}$ : 90.5% 434/89.8% 614/90.8% 723	Mo	10.15d $^{92m}\text{Nb}$ : 99% 934.5/0.90% 1847 34.97d $^{95}\text{Nb}$ : 0.028% 204/99.8% 766 62d $^{91m}\text{Nb}$ : 0.56% 105/-4% 1205 64d $^{95}\text{Zr}$ : 44.1% 724/54.5% 757 83.4d $^{88}\text{Zr}$ : 97.3% 393 20.3Ky $^{94}\text{Nb}$ : 99.8% 703/99.9% 871
Al	0.72My $^{26}\text{Al}$ : 99.76% 1809	Re	38d $^{184}\text{Re}$ : 17.1% 111/3.0% 253/1.9% 642/37.5% 792/15.5% 895/38.1% 903/0.5% 1023 75.1d $^{185}\text{W}$ : 0.019% 125 115d $^{182}\text{Ta}$ : 34.7% 1121/16.5% 1189/27.3% 1221/ 11.6% 1231/ 1.4% 1289 165d $^{184m}\text{Re}$ : 13.3% 105/5.9% 111/6.6% 161/2.8% 215/9.6% 217/1.5% 227/10.9% 253/ 5.9% 318/3.2% 384/3.4% 537/3.8% 792/ 2.8% 895/3.8% 903/8.4% 921/1.2% 1174 0.2My $^{186m}\text{Re}$ : not seen (1.19% 99.39)
Dy	72.3d $^{160}\text{Tb}$ : 5.2% 197/4.0% 216/26.8% 299/2.0% 765/29.8% 879/9.8% 962/25% 966/15.2% 1178/7.5% 1272/2.9% 1312 150y $^{158}\text{Tb}$ : 43% 944	Tb	72.3d $^{160}\text{Tb}$ : 26.8% 299/29.8% 879/9.8% 962/25% 966/15.2% 1178/7.5% 1272/2.9% 1312 150y $^{158}\text{Tb}$ : 5.6% 99/9.2% 182/0.93% 218/9.3% 780/4.3% 944/ 19.8% 962/2.1% 1108/1.7% 1187
Eu	8.8y $^{154}\text{Eu}$ : 19.7% 723/11.5% 873/10.3% 996/17.9% 1005/35.5% 1275 13.3y $^{152}\text{Eu}$ : 28.4% 122/7.5% 245/26.6% 344/13% 779/4.2% 867/14.5% 964/9.9% 1086/13.6% 1112/1.6% 1299/20.8% 1408 35.8y $^{150}\text{Eu}$ : 94% 334/78.7% 439/4.7% 505/51.5% 584/9.4% 737/5.1% 748/5.2% 1049/1.9% 1247/2.5% 1344	W	75.1d $^{185}\text{W}$ : 0.019% 125 115d $^{182}\text{Ta}$ : 34.7% 1121/16.5% 1189/27.3% 1221/ 11.6% 1231/ 1.4% 1289 121.2d $^{181}\text{W}$ : 0.032% 136/0.084% 152 31y $^{178m2}\text{Hf}$ : not seen
Hf	25.1d $^{179m2}\text{Hf}$ : 65% 454 KeV 42.4d $^{181}\text{Hf}$ : 80.6% 482 70d $^{175}\text{Hf}$ : 87% 343/1.6% 433 1.37y $^{173}\text{Lu}$ : 3.1% 101/1.8% 171/0.83% 179/13% 272/0.35% 285/0.3% 557/0.87% 636 31y $^{178m2}\text{Hf}$ : 81.1% 213/63.8% 217/16.6% 258/94.1% 326/97.1% 426/ 68.9% 495/ 83.7% 574 From Zr impurity: 64d $^{95}\text{Zr}$ : 44.1% 724/54.5% 757		
Ir	73.83d $^{192}\text{Ir}$ : 3.2% 206/28.3% 296/29.3% 308/83% 317/47.7% 468/3.1% 485/4.5% 589/8.2% 604/5.3% 612 171d $^{194m}\text{Ir}$ : 93% 328/97% 483/59% 688/3.6% 1012 241y $^{192m}\text{Ir}$ : not seen (0.097% 115)		

III. HIGHLIGHTS OF MEASURED AND TREATED DATA

Foils were weighed before irradiation, and their masses were determined within 0.1%. Foil mass and count time are used as input for obtaining the decay  $\gamma$  emission rate from measured counts. The peak-wise count data was treated to obtain decay  $\gamma$  emission rate per g for a normalizing source neutron intensity of

$10^{12}$  n/s. Figure 3 shows total, integrated (100 KeV to 3 MeV  $\gamma$ -energy)  $\gamma$ -emission rate as a function of Z of irradiated material for cooling times listed in Tab.II. Note that EU1 and EU3 stand respectively for 97.7%  $^{151}\text{Eu}$  enriched and 99.2%  $^{153}\text{Eu}$  enriched europium. It is interesting to observe that decay  $\gamma$  rate is quite low for Al and it hits a peak, for a value of  $\sim 10^4$   $\gamma$ s per g, for EU3, and then starts dropping and hits minimum at Dy. It starts rising

TABLE IV

Reactions Contributing to Observed  $\gamma$ -Ray Peaks

Sample	Radioactive Isotopes	Reactions	Sample	Radioactive Isotopes	Reactions
Ag	$^{108}\text{Ag}$	IT $^{108}\text{mAg} \rightarrow ^{108}\text{Ag}$ $^{108}\text{Ag} \rightarrow ^{108}\text{Ag}$ $^{109}\text{Ag}(n,2n)^{108}\text{mAg}; ^{107}\text{Ag}(n,\gamma)^{108}\text{mAg}$ $^{109}\text{Ag}(n,\gamma)^{110}\text{mAg}$	Ir	$^{192}\text{Ir}$	IT $^{192}\text{Ir}(n,2n)^{192}\text{Ir}; ^{191}\text{Ir}(n,\gamma)^{192}\text{Ir}; ^{192}\text{mIr} \rightarrow ^{192}\text{Ir}$ $^{241}\text{y}$
	$^{108}\text{mAg}$ $^{110}\text{mAg}$			$^{194}\text{mIr}$	
Al	$^{26}\text{Al}$	$^{27}\text{Al}(n,2n)^{26}\text{Al}$	Mo	$^{92}\text{mNb}$	$^{92}\text{Mo}(n,p)^{92}\text{mNb}; ^{94}\text{Mo}(n,\alpha)^{92}\text{mNb}$ $^{95}\text{Nb}$ $^{95}\text{Mo}(n,p)^{95}\text{Nb}; ^{95}\text{mNb}(T/87h) \rightarrow ^{95}\text{Nb}; ^{94}\text{Mo}(n,\alpha)^{95}\text{Nb}$ $^{92}\text{Mo}(n,\alpha)^{91}\text{mNb}$ $^{92}\text{Zr}$ $^{88}\text{Zr}$ $^{94}\text{Nb}$
Dy	$^{160}\text{Tb}$ $^{158}\text{Tb}$	$^{160}\text{Dy}(n,p)^{160}\text{Tb}; ^{161}\text{Dy}(n,\alpha)^{160}\text{Tb}; ^{162}\text{Dy}(n,\alpha)^{160}\text{Tb};$ IT $^{160}\text{Dy}(n,\alpha)^{158}\text{Tb}; ^{160}\text{Dy}(n,\alpha)^{158}\text{mTb} \rightarrow ^{158}\text{Tb};$ $^{160}\text{Dy}(n,\alpha)^{158}\text{Tb}; ^{160}\text{Dy}(n,\alpha)^{158}\text{mTb}$ $^{160}\text{Dy}(n,\alpha)^{158}\text{Tb}; ^{160}\text{Dy}(n,\alpha)^{158}\text{mTb}$ $^{158}\text{Dy}(n,p)^{158}\text{mTb}$		$^{94}\text{Mo}(n,p)^{94}\text{Nb}; ^{94}\text{mNb}(T/6.3m) \rightarrow ^{94}\text{Nb}; ^{92}\text{Mo}(n,\alpha)^{94}\text{Nb};$ $^{96}\text{Mo}(n,\alpha)^{94}\text{Nb}; ^{96}\text{Mo}(n,\alpha)^{94}\text{Nb}$	
Eu	$^{154}\text{Eu}$ $^{152}\text{Eu}$	$^{153}\text{Eu}(n,\gamma)^{154}\text{Eu}$	Re	$^{184}\text{Re}$ $^{185}\text{W}$	$^{183}\text{Re}(n,2n)^{184}\text{Re}; ^{184}\text{mRe}(T/1.65d) \rightarrow ^{184}\text{Re}$ $^{183}\text{Re}(n,p)^{183}\text{W}$ $^{185}\text{Re}(n,2n)^{184}\text{Re}$ $^{185}\text{Re}(n,\alpha)^{182}\text{Ta}$
	$^{150}\text{Eu}$	$^{152}\text{Eu}(n,2n)^{152}\text{Eu}; ^{151}\text{Eu}(n,\gamma)^{152}\text{Eu}; ^{152}\text{mEu} \rightarrow ^{152}\text{Eu}$ IT $^{152}\text{Eu}(n,2n)^{150}\text{Eu}$		$^{182}\text{Ta}$	
Hf	$^{179\text{m}}\text{Hf}$ $^{175}\text{Hf}$ $^{173}\text{Lu}$	$^{180}\text{Hf}(n,2n)^{179\text{m}}\text{Hf}; ^{179}\text{Hf}(n,\alpha)^{179\text{m}}\text{Hf}; ^{178}\text{Hf}(n,\gamma)^{179\text{m}}\text{Hf}$ $^{176}\text{Hf}(n,2n)^{175}\text{Hf}; ^{174}\text{Hf}(n,\gamma)^{175}\text{Hf}$ $^{174}\text{Hf}(n,\alpha)^{173}\text{Lu}$ $^{72}\text{Hf}(n,\alpha)^{71}\text{Lu}$	Tb	$^{160}\text{Tb}$ $^{158}\text{Tb}$	$^{159}\text{Tb}(n,\gamma)^{160}\text{Tb}$ $^{159}\text{Tb}(n,2n)^{158}\text{Tb}; ^{158}\text{mTb}(T/10.5s) \rightarrow ^{158}\text{Tb}$
	$^{178\text{m}}\text{Hf}$ $^{181}\text{Hf}$	$^{179}\text{Hf}(n,2n)^{178\text{m}}\text{Hf}; ^{178}\text{Hf}(n,\alpha)^{178\text{m}}\text{Hf}; ^{177}\text{Hf}(n,\gamma)^{178\text{m}}\text{Hf}$ $^{180}\text{Hf}(n,\gamma)^{181}\text{Hf}$		W	

dominates the decay rate. It accounts for ~76% of total.

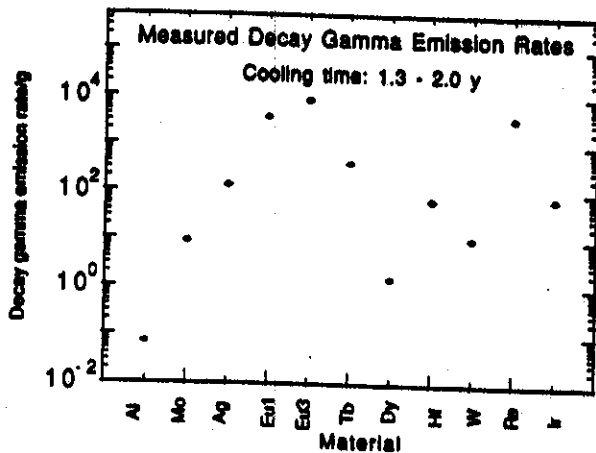


Fig. 3. Measured  $\gamma$ -energy integrated (100 Kev- 3MeV) decay  $\gamma$ -emission rates as a function of material, the latter being arranged in order of increasing Z

again and hits a small peak at hafnium. Tungsten shows a relative decrease and lies at second minimum. Rhenium lies at top of third peak. It is to be stressed that this behavior is essentially characteristic of cooling times covered.

Material-wise highlights are summarized as follows:

III.A. Aluminum & Silver

Only one isotope, e.g.,  $^{26}\text{Al}$ , has been identified in aluminum. The decay rate is one of the lowest. Even after counting time of 13946.m (9.7d), net error on decay rate is ~25%. Two isotopes,  $^{108}\text{mAg}$  and  $^{108}\text{Ag}$ , have been identified for silver. All prominent peaks have low statistical error.  $^{108}\text{mAg}$

III.B. Molybdenum

The dominant isotopes are  $^{95}\text{Nb}$ , and  $^{95}\text{Zr}$ . The other isotopic activities are for  $^{91}\text{mNb}$ ,  $^{88}\text{Zr}$ , and  $^{94\text{m}+8}\text{Nb}$ .  $^{95}\text{Nb}$  accounts for 58.9%,  $^{95}\text{Zr}$  for 26.3%, and,  $^{94}\text{Nb}$  for 0.8%. The total error on  $^{94\text{m}+8}\text{Nb}$  decay rate is ~22%.

III.C. Dysprosium & Terbium

Only two isotopes have been identified in dysprosium, e.g.,  $^{160}\text{Tb}$ , and  $^{158\text{m}+8}\text{Tb}$ .  $^{160}\text{Tb}$  accounts for as much as 96% of total decay rate. Also, counting statistics for  $^{158}\text{Tb}$  are quite poor, the net error being ~67%.

Terbium too has two products, i.e.,  $^{158}\text{Tb}$ , and  $^{160}\text{Tb}$ . However,  $^{158}\text{Tb}$  dominates by far and accounts for as much as ~88% of the total decay rate. Moreover, the counting error is quite low, almost on all identified peaks for both the isotopes.

III.D. Europium

For 97.7%  $^{151}\text{Eu}$ -enriched foil, only two products were observed, e.g.,  $^{150}\text{Eu}$ , and  $^{152\text{m}+8}\text{Eu}$ .  $^{150}\text{Eu}$  decay rate dominates the total, being as much as 75%. However, ~25% contribution by  $^{152}\text{Eu}$  is alarming as it highlights the effectiveness of softer component of the neutron energy spectrum during radiative capture, i.e.,  $^{151}\text{Eu}(n,\gamma)^{152}\text{Eu}$ . By the same token, analytical modeling of the experiment will have to try to account for all sources of neutron slowing down.

99.2%  $^{153}\text{Eu}$ -enriched foil brings out three identifiable contributors, e.g.,  $^{152\text{m}+8}\text{Eu}$ ,  $^{154}\text{Eu}$ , and  $^{150}\text{Eu}$ .  $^{152}\text{Eu}$  dominates with 95.2%, and  $^{154}\text{Eu}$  and  $^{150}\text{Eu}$  follow up with 4.1 and 0.7% respectively.  $^{153}\text{Eu}(n,\gamma)^{154}\text{Eu}$  appears to have less effective cross-section as compared to that for  $^{151}\text{Eu}(n,\gamma)^{152}\text{Eu}$ .

### III.E. Hafnium

$^{175}\text{Hf}$  dominates energy-integrated decay rate. It accounts for almost 81%. Other contributors are:  $^{173}\text{Lu}$  (12%),  $^{178\text{m}2}\text{Hf}$  (5.4%), and  $^{95}\text{Zr}$  (1%).  $^{179\text{m}2}\text{Hf}$  contributes ~0.25% only. Note that  $^{95}\text{Zr}$  ( $t_{1/2}=64\text{d}$ ) results from 2.8% Zr impurity in hafnium sample.

### III.F. Rhenium & Tungsten

In rhenium,  $^{184\text{m}}\text{Re}$  accounts for as much as 95% of total, followed by  $^{184}\text{Re}$  (1.6%), and  $^{182}\text{Ta}$  (0.2%). However, 0.2My  $^{186\text{m}}\text{Re}$  decay  $\gamma$ 's at 99.4 KeV were not observed.

Leading contributor in decay rate of irradiated tungsten sample is  $^{182}\text{Ta}$ , giving as much as 86.4%. Most of the remaining contribution comes from  $^{185}\text{W}$ . One of the counting runs saw faint twin peaks of  $^{181}\text{W}$ , i.e., at 136 and 152 KeV. The counting error is more than 30% at each of these two peaks, however.

### III.G. Iridium

Only two contributors were identifiable. These are  $^{192}\text{Ir}$  and  $^{194\text{m}}\text{Ir}$ . However,  $^{194\text{m}}\text{Ir}$  accounts for only 1.8%, as against 98.2% for  $^{192}\text{Ir}$ . This kind of trend is expected in a hard, 14MeV dominated neutron energy spectrum. No trace of 115 KeV peak of  $^{241}\text{y}$   $^{192\text{m}}\text{Ir}$  was to be found in the measured  $\gamma$ -spectrum.

## IV. ANALYSIS

As described in Ref. 16, analysis involves a multi-step procedure. Neutron energy spectrum was computed for all foils in foil package#1 with MCNP<sup>20</sup> for irradiation geometry shown in Figs. 1 and 2. Wherever possible, RMCCS evaluation was used for transport cross-sections. Energy-dependent branching ratio between  $^{92\text{m}}\text{Nb}$  and  $^{92}\text{Nb}$  was used to obtain correct  $^{93}\text{Nb}(n,2n)^{92\text{m}}\text{Nb}$  reaction rate. Figure 4 displays a typical MCNP evaluated neutron energy spectrum, for first Nb foil.

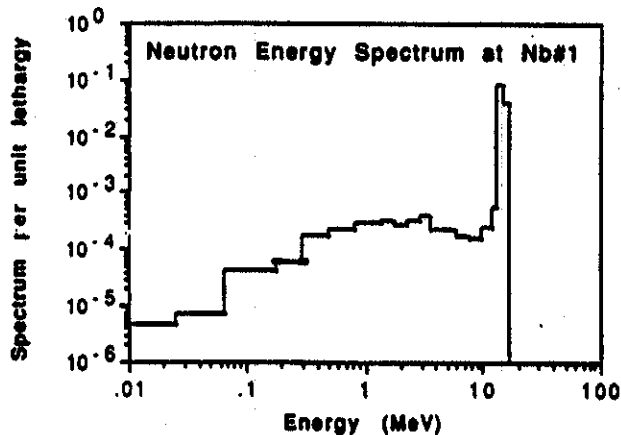


Fig. 4. Computed neutron energy spectrum, by MCNP, at first Nb foil location in package#1

Also,  $^{93}\text{Nb}(n,2n)^{92\text{m}}\text{Nb}$  reaction rates were computed at all ten Nb foil locations. These computed  $^{92\text{m}}\text{Nb}$  production rates were compared to measured rates and a correction factor was obtained for computed neutron energy spectrum for each foil location. The corrected neutron energy spectra were then used to generate multi-group fluxes for each of four leading radioactivity codes, e.g.,

DKRICF<sup>21</sup>, REAC-2<sup>22</sup>, RACC<sup>23</sup>, and ACT4 (central THIDA-2 module)<sup>24</sup>. Overall neutron flux conservation was governing criterion for this transformation. Discrepancy between transformed and original flux was computed to be negligible. Other input parameters for these codes included sample composition, irradiation and cooling times. Decay and activation cross section libraries form part of each code used.

The decay data and cross-section libraries of these four codes were searched to find the existence of data for all nuclides of interest for the reported measurements. Only REAC-2 contains most of the data. There is no data for  $^{158}\text{Dy}$  reactions. It is for this reason that  $^{158}\text{Dy}(n,p)^{158\text{m}}\text{Tb}$  reaction for  $^{158}\text{Tb}$  product of Dy has been enclosed within square brackets in Tab. IV. RACC libraries were the most deficient of the remaining three. RACC has no data for Ag, Dy, Eu, Hf, Ir, Re, and Tb. DKRICF (or, mentioned interchangeably, DKR) has no data for Dy, Hf, Ir, and Tb. Also, a number of times, data is incomplete even for the cases where it exists, e.g., there is no data for  $^{185}\text{Re}(n,\gamma)^{186\text{m}}\text{Re}$ ,  $^{185}\text{Re}(n,\alpha)^{182}\text{Ta}$ , and  $^{187}\text{Re}(n,2n)^{186\text{m}}\text{Re}$ . THIDA-2 has no data for Dy, Ir, and Tb. Also, it is not as complete as REAC-2 libraries for other materials.

We have followed two-pronged approach during analysis. Evaluated spectra of decay  $\gamma$  emission rates were compared to those measured, on one hand, and deduced experimental reaction rates (by using published decay  $\gamma$ -yields from Ref. 18) were also compared to those computed by these codes, on the other hand. A number of these calculations were cross-checked by an independent calculation using all required data from data libraries of each code. Good agreement was found between the two. In what follows, an attempt has been made to compare reaction rates rather than decay  $\gamma$ -rates. This is to avoid pitfalls related to elementary errors committed by the people typing in the decay data libraries of these codes. In fact, we discovered quite a number of such instances during our concurrent work on short-lived isotopes 15-16. Correct decay data was assured for all calculations for same target-product combination in the current analysis.

## V. RESULTS AND DISCUSSION

Figures 5 through 14 show ratio of computed (C) to experimentally (E) measured reaction rates for the identified products for all eleven foils of package#1. Each figure displays C/E's for all codes having nuclear data for the products involved. Name of each isotope is entered close to one of the C/E's. Cooling time is also mentioned.

For  $^{108\text{m}}\text{Ag}$  (see Fig. 5), C/E's for different codes are: REAC, 2.19 (6% error); DKRICF, 2.19(6%); THIDA, 3.69 (6%). For  $^{110\text{m}}\text{Ag}$ , C/E's are: REAC, 0.39; DKRICF, 0.35; THIDA,  $1.85 \cdot 10^{-2}$ . The cross-sections at 14 MeV in all the libraries need major revisions for  $^{108\text{m}}\text{Ag}$  production. Using recently reported measured cross-section<sup>14</sup>, one gets the following ratio of the library data to the measurement at 14 MeV: REAC, 1.9; DKRICF, 1.9; THIDA, 3.2. In this regard, it is important to mention that recent PTB measurements yield  $^{108\text{m}}\text{Ag}$  half life of  $\sim 300\text{y}$ . Our analysis assumed half life of 127y. If we accept new value of half life of  $\sim 300\text{y}$ , modified C/E ratios for  $^{108\text{m}}\text{Ag}$  are: REAC, 0.93 (6%); DKRICF, 0.93 (6%); THIDA, 1.56 (6%). This leads to important inference that the cross-sections in REAC-2 and DKRICF are within acceptable statistical error. But one needs to modify  $^{108\text{m}}\text{Ag}$  half life to  $\sim 300\text{y}$ . Before this inference is accepted by us, we will verify this by new measurements on Ag foil at zero degree in identical foil-detector configuration.

For  $^{26}\text{Al}$ , C/E's are: REAC, 1.17 (26%); DKRICF, 0.62 (26%); THIDA, 0.19 (26%); RACC, 0.25 (26%). Dysprosium

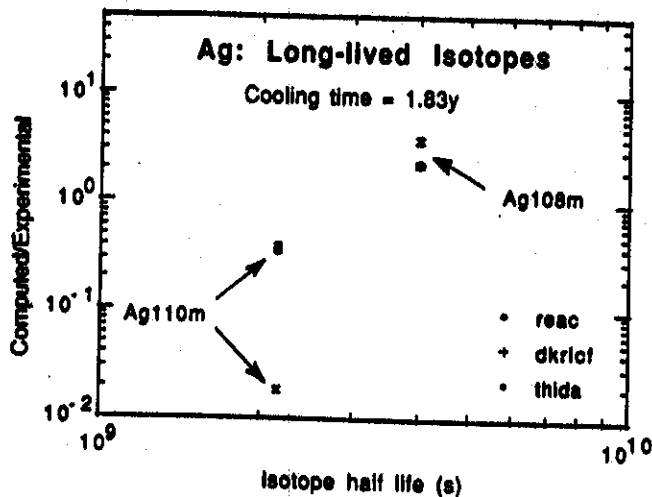


Fig. 5. Ag: ratio of computed(C) to experimentally measured (E) activation rates as a function of product half life

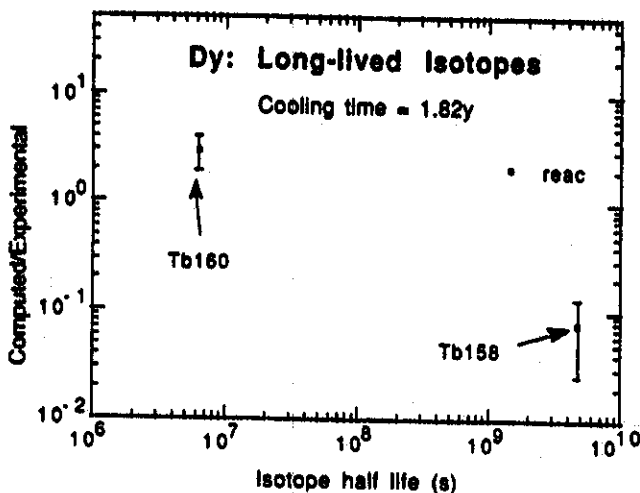


Fig. 6. Dy: ratio of computed(C) to experimentally measured (E) activation rates as a function of product half life

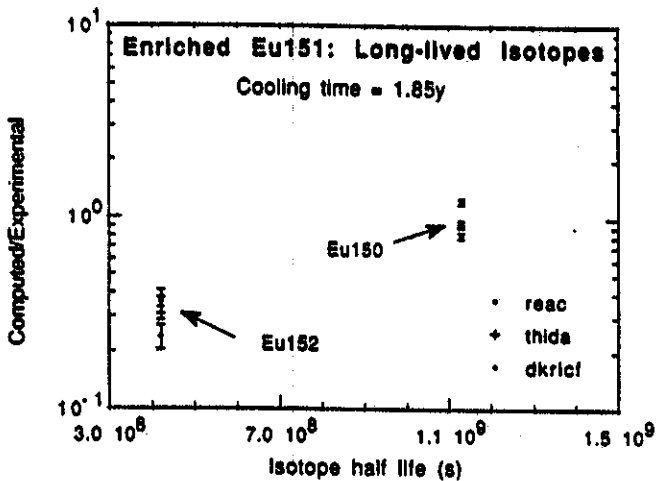


Fig. 7. 97.7% <sup>151</sup>Eu -enriched Europium: ratio of computed(C) to experimentally measured (E) activation rates as a function of product half life

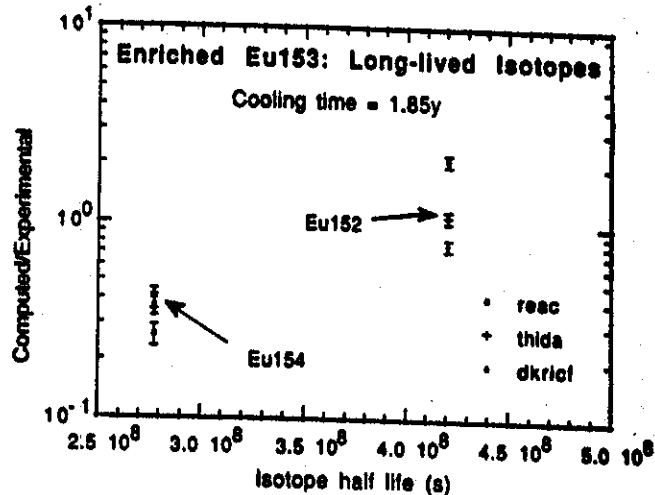


Fig. 8. 99.2% <sup>153</sup>Eu -enriched Europium: ratio of computed(C) to experimentally measured (E) activation rates as a function of product half life

(see Figure 6) has poor counting statistics. <sup>158m+s</sup>Tb and <sup>160</sup>Tb yield C/E's of 7.78.10<sup>-2</sup> (67%), and 2.91 (35%) respectively, by REAC-2. Main reason for low C/E for <sup>158m+s</sup>Tb is to be found in missing cross-section data on <sup>158</sup>Dy(n,p)<sup>158m+s</sup>Tb reactions in REAC-2.

<sup>151</sup>Eu-enriched europium has low C/E for <sup>152</sup>Eu (see Figure 7). Partly, it might come from lack of enough accounting for low energy neutrons as cross section for <sup>151</sup>Eu(n,γ)<sup>152</sup>Eu picks up rapidly at lower neutron energies. In fact, it is a tough problem to accumulate acceptable statistics, with MCNP, after accounting for all details of the experimental geometry. Too many geometrical cells will exorge exorbitant CPU time. C/E's for <sup>150</sup>Eu production are: REAC, 1.23 (4%); DKRICF, 0.81 (4%); THIDA, 0.94 (4%). Discrepancy for <sup>150</sup>Eu is traceable to inaccurate cross-section data in REAC-2 and DKRICF. Using measured data<sup>14</sup> at 14 MeV as normalization, one obtains the following ratios for the library cross-sections: REAC, 1.42; DKRICF, 0.85; THIDA, 0.99.

<sup>153</sup>Eu-enriched europium has low C/E for <sup>154</sup>Eu (see Figure 8). C/E for <sup>152s+m</sup>Eu product gives a lot of divergence among different codes. C/E's for this isotope are: REAC, 2.14 (7%); DKRICF, 0.79 (7%); THIDA, 1.10 (7%). The source of divergent C/E's for <sup>152m+s</sup>Eu lies in discrepant cross-section data for all the libraries. Normalizing with respect to measured data of Ref. 14, one obtains the following ratios for the library cross-section at 14 MeV: REAC, 2.26; DKRICF, 0.79; THIDA, 1.11. REAC-2 has same cross-section for metastable and ground states of the product, i.e., 1.88b. But, THIDA shows only 23.2% of total cross-section of 1.85b being in the metastable state. In fact, REAC-2 has simplified 50%-50% division into ground and metastable states for almost all the radioactive products. The present case is no exception.

Hafnium results look 'relatively good' for <sup>179m2</sup>Hf and <sup>175</sup>Hf only (see Fig. 9). C/E for <sup>179m2</sup>Hf is 1.21 (15%) by REAC-2. Other codes do not have cross-section data for the generating reactions. C/E's for <sup>175</sup>Hf are: REAC, 1.94 (5%); THIDA, 1.88 (5%). There is no data in THIDA for prediction of <sup>173</sup>Lu. REAC-2 does not do much better. C/E is just 4.51.10<sup>-5</sup> (2%)! Again, there is no explicit mention of data for <sup>178m2</sup>Hf in THIDA. REAC-2 yields a C/E of 377.42 (8%) for the same product. In fact, cross section at 14 MeV for the reaction leading to the production of this isotope, in REAC-2 library, is 2.07 b.

instead of measured value reported<sup>14</sup> in the range of 6.3(10%) mb!

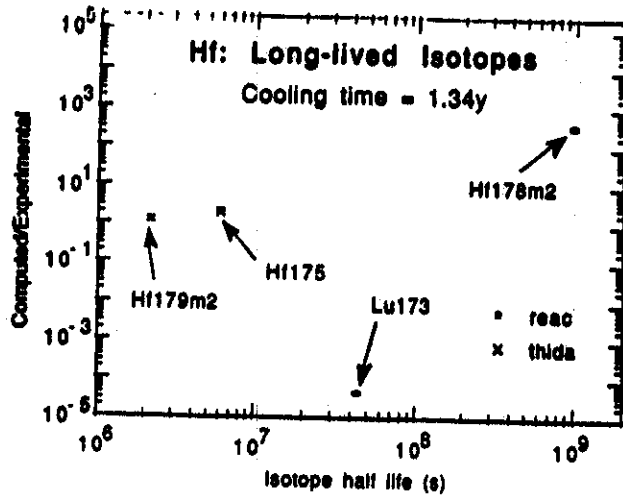


Fig. 9. Hf: ratio of computed(C) to experimentally measured (E) activation rates as a function of product half life

Iridium has large C/E for <sup>194m</sup>Ir (see Fig. 10). It is 103.52 (38% error). DKRICF lacks basic data for prediction of this isotope. <sup>192</sup>Ir is predicted pretty closely by REAC-2 and DKRICF; C/E's are: REAC, 1.20 (2.6%); DKRICF, 1.26 (2.6%).

Molybdenum shows a big scatter in C/E's for 3 isotopes out of 5 (Fig. 11). Closest agreement among codes is found for <sup>95</sup>Zr (DKRICF: 0.87, THIDA: 0.94), and <sup>95</sup>Nb (DKRICF: 0.92, THIDA: 0.92). C/E's for <sup>94</sup>Nb are: REAC, 2.62 (21%); DKRICF, 1.56; THIDA, 0.59; RACC, 0.39; Compared to measured value<sup>14</sup> at 14 MeV, one finds the same trends for the library cross-section data for <sup>94</sup>Nb production as for the  $\gamma$ -decay rates.

Rhenium has comparable C/E's from REAC and THIDA for <sup>182</sup>Ta (Fig. 12). The C/E's are: REAC, 0.78 (26%); THIDA, 0.67 (26%). DKRICF does not have <sup>185</sup>Re(n, $\alpha$ )<sup>182</sup>Ta cross-section. <sup>184m</sup>Re has C/E's varying as: REAC, 0.68 (2.6%); DKRICF, 0.68 (2.6%); THIDA, 1.54 (2.6%).

Terbium has C/E's from REAC-2 alone (Fig. 13), as nuclear data for it is missing in other codes. C/E's for <sup>160</sup>Tb and <sup>158m+s</sup>Tb are respectively 0.63 (11%), and 2.01 (3.2%). C/E looks surprisingly respectable for <sup>158m+s</sup>Tb! Here again, the total cross-section data at 14 MeV for <sup>159</sup>Tb(n,2n)<sup>158m+s</sup>Tb, in REAC-2, is overestimated by a factor of 2.19 vis-a-vis the recently reported measured data<sup>14</sup>.

Tungsten shows good agreement for <sup>181</sup>W (Fig. 14) among all four libraries. C/E's are: REAC, 2.79; DKRICF, 2.68; THIDA, 2.68; RACC, 2.85. However, things get bad for <sup>182</sup>Ta and <sup>185</sup>W. C/E's for <sup>182</sup>Ta are: REAC, 1.02 (8%); DKRICF, 0.74; THIDA, 1.01; RACC, 0.68. C/E's for <sup>185</sup>W are: REAC, 59.04 (26%); DKRICF, 46.88 (26%); THIDA, 57.37; RACC, 70.99.

Figure 15 is an attempt to summarize the status of evaluated versus measured data, irrespective of any code in particular, for products with half lives ranging from 0.68 y

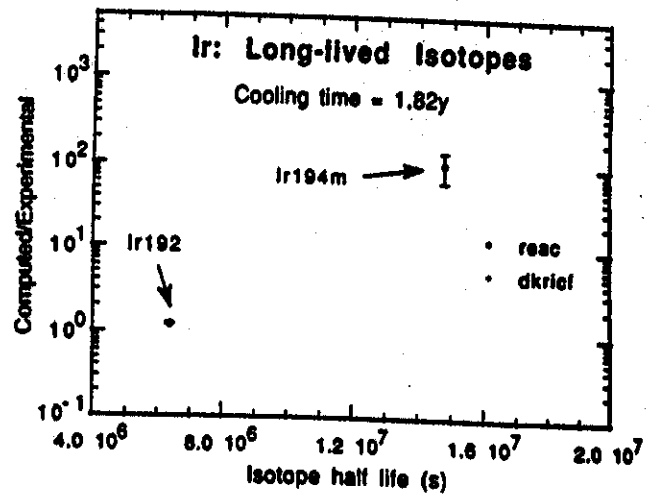


Fig. 10. Ir: ratio of computed(C) to experimentally measured (E) activation rates as a function of product half life

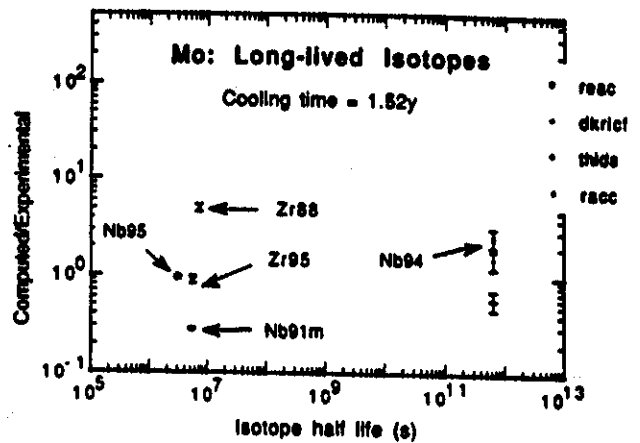


Fig. 11. Mo: ratio of computed(C) to experimentally measured (E) activation rates as a function of product half life

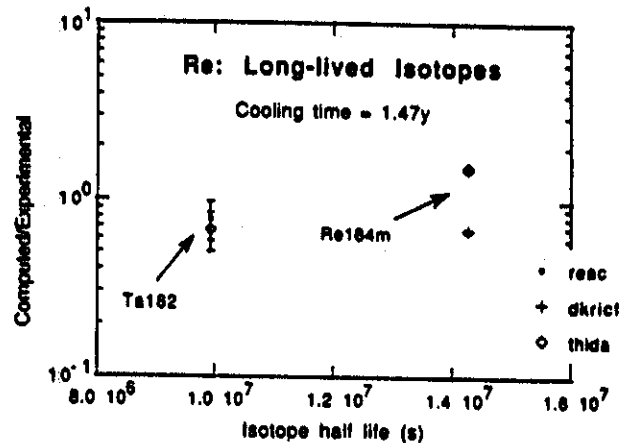


Fig. 12. Re: ratio of computed(C) to experimentally measured (E) activation rates as a function of product half life

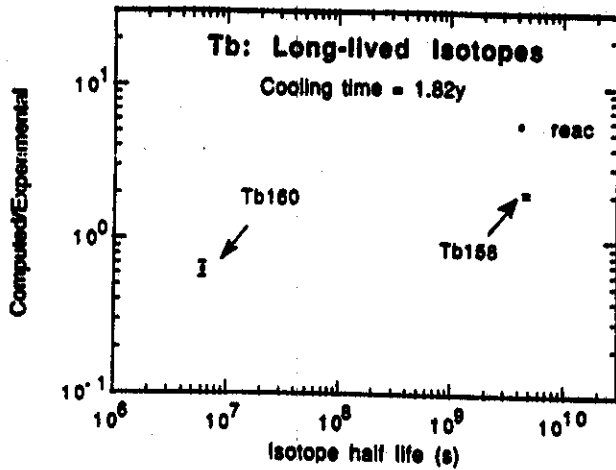


Fig. 13. Tb: ratio of computed(C) to experimentally measured (E) activation rates as a function of product half life

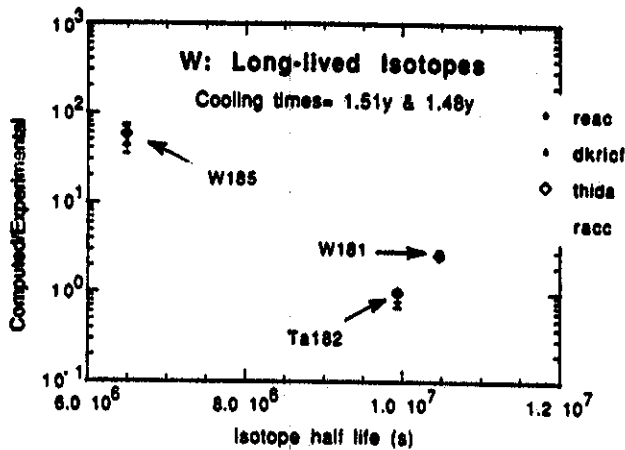


Fig. 14. W: ratio of computed(C) to experimentally measured (E) activation rates as a function of product half life

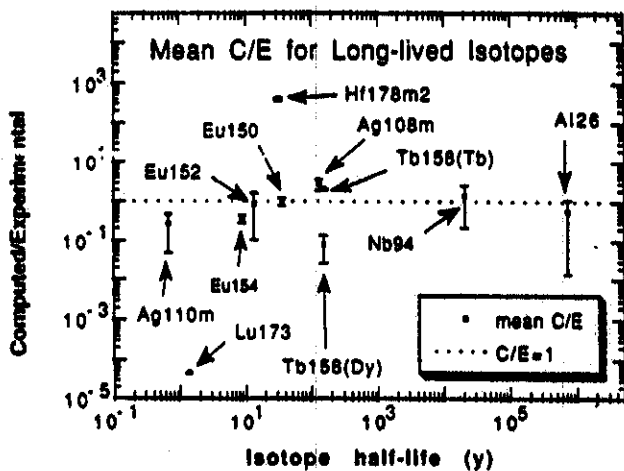


Fig. 15. Mean ratio of computed(C) to experimentally measured (E) activation rates as a function of product half life for half lives ranging from 0.68 y to 0.72 My

( $^{110m}\text{Ag}$ ) to 0.72 My ( $^{26}\text{Al}$ ). Mean C/E was evaluated from all available C/E's for each isotope. Ten isotopes are included. Also shown in the figure is C/E=1 line- a desired objective. Only  $^{150}\text{Eu}$ ,  $^{152}\text{Eu}$ ,  $^{94}\text{Nb}$ , and  $^{26}\text{Al}$  come closest to this line, even though uncertainty on all data except for  $^{150}\text{Eu}$  is quite staggering. Generally, the data falls on both sides of this C/E=1 line.  $^{178m2}\text{Hf}$  is strongly overpredicted,  $^{108m}\text{Ag}$  and  $^{158m+s}\text{Tb}$  (from Tb) are significantly overpredicted,  $^{173}\text{Lu}$  and  $^{158m+s}\text{Tb}$  (from Dy) are strongly underpredicted. Underprediction of  $^{110m}\text{Ag}$ , and  $^{154}\text{Eu}$  might be partly due to possible underestimation of softer component of the neutron energy spectrum used in the analysis. One needs to have in-depth verification through accumulation of additional experimentally experimental data is compiled, onus for revision of the cross sections falls on shoulders of the cross-section community.

VI. CONCLUSIONS

Experimental measurements of decay  $\gamma$  activity from long-lived products of eleven materials, subjected to an average fluence of  $\sim 0.83 \times 10^{15}$  n/cm<sup>2</sup> at FNS, under USDOE/IAERI collaborative program, have provided very valuable data for validation of largely untested, yet frequently used, leading radioactivity calculation codes employed by fusion reactor designers. Only REAC-2 has almost complete data-base, even though ratio of computed to measured activation rates departs from 1.0 for many products. RACC code has the narrowest data base- data being present for Al, Mo and W only. DKRICF and THIDA have partially complete data bases. On average, none of the codes seems to outdo others. C/E's for all eleven materials have been presented and discussed.

C/E ranges from  $4.10^{-5}$  to 377. Also, mean C/E, for isotopes with half life larger than 0.6 y, shows a spread extending on both sides of C/E=1.0.  $^{178m2}\text{Hf}$  is strongly overestimated (by a factor of 377) in REAC-2, and  $^{173}\text{Lu}$  ( $C/E=4.5 \cdot 10^{-5}$ ), and  $^{158m+s}\text{Tb}$  (from Dy) are strongly underestimated by the same code.  $^{108m}\text{Ag}$  and  $^{158m+s}\text{Tb}$  (from Tb) are significantly overpredicted. Only  $^{152}\text{Eu}$ ,  $^{150}\text{Eu}$ ,  $^{94}\text{Nb}$ , and  $^{26}\text{Al}$  come closest to C/E=1, even though the uncertainty is quite large. Partial explanation for underprediction of  $^{110m}\text{Ag}$ , and  $^{154}\text{Eu}$  might lie in possible underestimation of softer component of neutron energy spectrum used in the analysis.

A serious doubt hangs over<sup>2</sup> half life of  $^{108m}\text{Ag}$  as included in all codes thus far. A value of 127 y is being currently used but some reported measurements indicate a half life of  $\sim 300\text{y}$ . We intend to accumulate more experimental data to verify this observation independently. Until then, we shall work with the current value. Cross-section data at higher neutron energies in REAC-2 needs a major revision for  $^{109}\text{Ag}(n,2n)^{108m}\text{Ag}$ ,  $^{158}\text{Dy}(n,p)^{158m+s}\text{Tb}$  (it is missing altogether),  $^{94}\text{Mo}(n,p)^{94}\text{Nb}$ ,  $^{151}\text{Eu}(n,2n)^{150}\text{Eu}$ ,  $^{153}\text{Eu}(n,2n)^{152m2+s}\text{Eu}$ ,  $^{179}\text{Hf}(n,2n)^{178m2}\text{Hf}$ , and  $^{159}\text{Tb}(n,2n)^{158m+s}\text{Tb}$ . THIDA needs to have completely missing cross-section data for Dy, Ir, and Tb.  $^{179}\text{Hf}(n,2n)^{178m2}\text{Hf}$  is also absent. In addition, major corrections are required for  $^{109}\text{Ag}(n,2n)^{108m}\text{Ag}$ ,  $^{27}\text{Al}(n,2n)^{26}\text{Al}$ ,  $^{94}\text{Mo}(n,p)^{94}\text{Nb}$ , and  $^{153}\text{Eu}(n,2n)^{152m2+s}\text{Eu}$ . DKRICF is quite incomplete too. The data for Dy, Hf, Ir, and Tb needs to be incorporated. In addition, isotopic Re cross-sections need to be complemented. Major corrections are required for  $^{109}\text{Ag}(n,2n)^{108m}\text{Ag}$ ,  $^{27}\text{Al}(n,2n)^{26}\text{Al}$ ,  $^{94}\text{Mo}(n,p)^{94}\text{Nb}$ ,  $^{151}\text{Eu}(n,2n)^{150}\text{Eu}$ , and  $^{153}\text{Eu}(n,2n)^{152m2+s}\text{Eu}$ . RACC possesses the least complete library. There is data only for Al, Mo, and W. The data for all remaining materials need to be incorporated. In addition, major corrections are needed for cross-sections for the following:  $^{27}\text{Al}(n,2n)^{26}\text{Al}$  and  $^{94}\text{Mo}(n,p)^{94}\text{Nb}$ .



There is a need to accumulate more experimental data from foils in packages #2 and #3. Once confirmatory experimental data from these additional foils is accumulated, the cross-section working groups will have to work on the revision of the cross section data libraries of these codes. In parallel, it is recommended that evaluators undertake new theoretical calculations, akin to those reported recently in reference 25, so as to obtain closer estimates of the activation cross sections for the production of long-lived isotopes.

As long-drawn-out procedures are involved in certification of theoretical evaluations for inclusion in updated nuclear data files, it is highly desirable to have adhoc updated files which will reflect the new measured data. It is important to do so at an early date as waste classification of fusion specific materials critically depends on the production cross sections, as well as the half lives and branching ratios, of the long-lived isotopes. In fact, the specific activity limits for shallow-land burial (vide 10CFR61, Class C waste) derived in Ref. 5 were based on cross section and other basic data present in REAC-2. As we report large disagreements between our experimental measurements and those evaluated using REAC-2 for many reactions, those specific activity limits will undergo large changes. Generally, poorly known production cross-section data for long-lived isotopes are expected to become a thorny issue in coming days because of their serious impact on search for low activation materials for fusion. Recently, we discovered<sup>26</sup> a peculiar non-1/v dependence for two  $^{14}\text{C}$  ( $t_{1/2}=5730$  y,  $\beta^-$  emitter) producing capture cross-sections, e.g.,  $^{17}\text{O}(n,\alpha)^{14}\text{C}$ , and  $^{13}\text{C}(n,\gamma)^{14}\text{C}$ , at neutron energy larger than 10KeV, in REAC-2 and DKRICF, during course of a low activation blanket design study for an inertial confinement fusion reactor. The design had a first wall made of SiC and tritium breeding region made of  $\text{Li}_2\text{O}$ . The initial computation with DKRICF classified the breeder region above class C, but a new calculation with modified cross sections based on Ref. 27 reclassified this region as class A. The impact of the kind of the measurements reported in this work on waste classification issues is quite apparent and it needs to be strengthened further.

#### ACKNOWLEDGEMENTS

This effort is supported by the United States Department of Energy, Office of Fusion Energy under Grant No. DE-F603-86ERS2124, and Japan Atomic Energy Research Institute.

#### REFERENCES

1. E.T. CHENG, "Radioactivity Aspects of Fusion Reactors," *Fusion Engineering and Design*, 10, 231 (1989).
2. E.T. CHENG, "Implications of the IAEA CRP on Long-lived Activation Cross Sections on Waste Disposal and Materials Recycling for Fusion Reactor Materials," presented at 1st IAEA Research Coordination Meeting on Activation Cross Sections for the Generation of Long-lived Radionuclides of Importance in Fusion Reactor Technology, Vienna, Austria, 11-12 November, 1991.
3. C. PONTI, "Fusion Reactor Materials to minimize Long-lived Radioactive Waste," *Fusion Engineering and Design*, 10, 243 (1989).
4. R.W. CONN et al., Report of the "DOE panel on Low Activation Materials for Fusion Applications, University of California, Los Angeles Report UCLA/PPG-728, June 1983; see also, R.W. CONN et al., "Lower Activation Materials and Magnetic Fusion Reactors," *Nucl. Technol./Fusion*, 5, 291 (1984).
5. S. FETTER et al., "Long-term Radioactivity in Fusion Reactors," *Fusion Engineering and Design*, 6, 123 (1988).

6. S.M. QAIM, "Recent Developments in Cross-section Measurements for Fusion Reactors," *Proc. of Int. Conf. on Nuclear Data for Science and Technology*, May 30-June 3, 1988, Mito, Japan, pp. 179-186, Edited by S. Igarasi, JAERI (1988).

7. E.T. CHENG, "Review of the Nuclear Data Status and Requirements for Fusion Reactors," *Proc. of Int. Conf. on Nuclear Data for Science and Technology*, May 30-June 3, 1988, Mito, Japan, pp. 187-192, Edited by S. Igarasi, JAERI (1988).

8. R.K. SMITHER, and L.R. GREENWOOD, "Measurement of the  $^{27}\text{Al}(n,2n)^{26}\text{Al}$  Reaction Cross Section for Fusion Reactor Applications," *Journal of Nuclear Materials*, 122&123, 1071 (1984).

9. L.R. GREENWOOD, D.G. DORAN, and H.L. HEINISCH, "Production of  $^{91}\text{Nb}$ ,  $^{94}\text{Nb}$ , and  $^{95}\text{Nb}$  from Mo by 14.5-14.8 MeV Neutrons," *Physical Review C*, 35, 1, 76 (1987).

10. L.R. GREENWOOD, "Recent Research in Neutron Dosimetry and Damage Analysis for Materials Irradiations," in Special Technical Publication 956(1988), American Society for Testing and Materials, Philadelphia.

11. D.L. BOWERS, and L.R. GREENWOOD, "Analysis of Long-lived Isotopes by Liquid Scintillation Spectrometry," *Journal of Radioanalytical Chemistry*, Articles, 1234, 2, 461 (1988).

12. L.R. GREENWOOD, and D.L. BOWERS, "Production of Long-lived Activities in Fusion Materials," *Journal of Nuclear Materials*, 155-157, 585 (1988).

13. S. IWASAKI, J.R. DUMAIS, and K. SUGIYAMA, "Measurement of the Cross Section for  $^{27}\text{Al}(n,2n)^{27}\text{Al}$  ( $T_{1/2}=7.16\times 10^5$  y) Reaction with Activation Technique around 14 MeV," *Proc. of Int. Conf. on Nuclear Data for Science and Technology*, May 30-June 3, 1988, Mito, Japan, pp. 295-297, Edited by S. Igarasi, JAERI (1988).

14. Y. IKEDA, A. KUMAR, and C. KONNO, "Measurements of Long-lived Activation Cross Sections by 14 MeV Neutrons at FNS," presented at *Int. Conf. on Nuclear Data for Science and Technology*, May 1991, Julich, Germany; see also same title and authors, p. 172, *Proc. of International Workshop on Fusion Neutronics*, June 7, 1991, Karlsruhe, JAERI-memo 03-305 (September 1991).

15. A. KUMAR et al., "Salient Features of Induced Radioactivity and Nuclear Heating Measurements and Analysis," p. 68, *Proc. of International Workshop on Fusion Neutronics*, June 7, 1991, Karlsruhe, JAERI-memo 03-305 (September 1991).

16. A. KUMAR, M.A. ABDU, Y. IKEDA, and T. NAKAMURA, "Analysis of Induced Activities related to Decay Heat in Phase IIC Experimental Assembly: USDOE/JAERI Collaborative Program on Fusion Neutronics Experiments," *Fusion Technol.*, 19, 1909 (1991).

17. Y. IKEDA et al., "Experimental Verification of the Current Data and Methods for Induced Radioactivity and Decay Heat Calculation in D-T Fusion Reactors," to appear in *Proc. of 2nd Int. Symp. on Fusion Nuclear Technology in Fusion Engineering and Design*, June 2-7, 1991, Karlsruhe, Germany.

18. E. BROWNE, and R.B. FIRESTONE, "Table of Radioactive Isotopes," editor, V.S. SHIRLEY, John Wiley & Sons, Inc., New York (1986).

19. C.M. LEDERER, and V. SHIRLEY, editors, "Table of Isotopes," 7th edition, John Wiley & Sons, Inc., New York (1978).

20. J.F. BREISMEISTER, editor, "MCNP- A General Monte Carlo Code for Neutron and Photon Transport: Version 3A," report no. LA-7396-M, Rev. 2 (Sep. 1988), along with MCNP3B newsletter dated July 18, 1988, Los Alamos National Laboratory.

21. D.L. HENDERSON and O. YASAR, "A Radioactivity and Dose Rate Calculation Code Package," Vol. 1 and 2, RSIC computer code collection, CCC-323 (April 1987).

22. F. M. MANN, "REAC\*2: Users Manual and Code Description," WHC-EP-0282, Westinghouse Hanford Company (1989).

23. J. JUNG, "Theory and Use of the Radioactivity Code RACC," ANL/FPP/ TM-122, Argonne National Laboratory (1979).

24. Y. SEKI et al., "THIDA-2: An Advanced Code System for Calculation of Transmutation, Activation, Decay Heat and Dose Rate," RSIC computer code collection, CCC-410 (April 1987).

25. M.B. CHADWICK, and P.G. YOUNG, "Calculations of the Production Cross Sections of High-Spin Isomeric States in Hafnium," *Nuclear Science and Engineering*, 108, 117 (1991).

26. A. KUMAR, "Impact of 'Poorly Known' Cross-sections for  $^{17}\text{O}(n,\alpha)^{14}\text{C}$  and  $^{13}\text{C}(n,\gamma)^{14}\text{C}$  Reactions on Waste-classification of Low Activation Blankets", UCLA memo dated Feb. 16, 1992, University of California, Los Angeles (Feb. 1992).

27. W.E. ALLEY, and R.M. LESSLER, "Neutron Activation Cross Sections," *Nuclear Data Tables*, 11, 621 (1973).